Science Advances
AAAS

Supplementary Materials for

Recovering quantum entanglement after its certification

Hyeon-Jin Kim *et al.*

Corresponding author: Young-Sik Ra, youngsikra@gmail.com

Sci. Adv. **9**, eadi5261 (2023)
DOI: 10.1126/sciadv.adi5261

This PDF file includes:

Supplementary Text
Figs. S1 to S6
References

Quantum process tomography of measurement operators

An arbitrary quantum operator in a two-dimensional Hilbert space can be characterized by a process matrix χ in the relation of $\mathcal{O}(\rho) = \Sigma_{m,n=1}^{4} \chi_{m,n} E_m \rho E_n^\dagger$, where ρ is an input state, and $\mathcal{O}(\rho)$ is the output state. As the basis operations, we choose $E_k = \{I, \sigma_x, \sigma_y, \sigma_z\}$. Using quantum process tomography (with the maximum likelihood estimation method (*41*)), we reconstruct the process matrix χ for each experimentally implemented operation.

Fig. S1 and S2 show the quantum process tomography results of weak measurement and reversal measurement, respectively. Fig. S3 shows the result of weak and reversal measurements when used together. We compare an experimentally implemented operation with a target quantum operator by calculating fidelity and purity, which are placed at the bottom of each figure.

Properties of the quantum state after weak measurement or after weak and reversal measurements

Fig. S4 shows the properties of the quantum state after weak measurement, and Fig. S5 shows the properties of the quantum state after weak and reversal measurements.

Improving reversibility by applying multiple reversal measurements

We discuss a method to enhance the reversibility by applying additional reversal measurements in the cases of unsuccessful recovery. Without loss of generality, we can start by considering the recovery of the weak measurement $\hat{M}^{(k)}_{+|\{p_k^{(1)}, \vec{s}_k\}}$ for $+1$ outcome, where $k = A, B$, and $p_k^{(1)}$ and $\vec{s}_k$ represent the measurement strength and direction, respectively. The successful recovery by a single application of the reversal measurement (as described in the main text) leads to the overall operation of $\hat{R}^{(k)}_{+|\{p_k^{(1)},\vec{s}_k\}} \hat{M}^{(k)}_{+|\{p_k^{(1)},\vec{s}_k\}} = \sqrt{r_k^{(1)}}\ \hat{I}$, where $\hat{I}$ is the identity operation indicating the successful recovery, and $r_k^{(1)}$ is the associated recovery probability. On the other hand, the unsuccessful recovery gives rise to the overall operation of $\hat{R}^{(k)}_{-|\{p_k^{(1)},\vec{s}_k\}} \hat{M}^{(k)}_{+|\{p_k^{(1)},\vec{s}_k\}}$.

This unsuccessful case can be further recovered by applying an additional reversal measurement $\hat{R}^{(k)}_{+|\{p_k^{(2)},\vec{s}_k\}}$, resulting in $\hat{R}^{(k)}_{+|\{p_k^{(2)},\vec{s}_k\}} \hat{R}^{(k)}_{-|\{p_k^{(1)},\vec{s}_k\}} \hat{M}^{(k)}_{+|\{p_k^{(1)},\vec{s}_k\}} = \sqrt{r_k^{(2)}}\ \hat{I}$ by choosing a proper strength of $p_k^{(2)}$. By generalizing this method, we obtain the overall operation of the successful recovery after applying n reversal measurements:

$$\hat{R}^{(k)}_{+|\{p_k^{(n)},\vec{s}_k\}} \left(\prod_{i=1}^{n-1} \hat{R}^{(k)}_{-|\{p_k^{(i)},\vec{s}_k\}} \right) \hat{M}^{(k)}_{+|\{p_k^{(1)},\vec{s}_k\}} = \sqrt{r_k^{(n)}}\ \hat{I}, \tag{S1}$$

where the proper choice of $p_k^{(n)}$ and the recovery probability $r_k^{(n)}$ are given by

$$\begin{aligned} p_k^{(n)} &= 1 - \frac{2}{1 + \left(\frac{1+p_k}{1-p_k}\right)^{2^{n-1}}} \\ r_k^{(n)} &= \frac{p_k}{2} \operatorname{csch}\left(2^{n-1} \ln\left(\frac{1+p_k}{1-p_k}\right)\right) \end{aligned} \tag{S2}$$

with $p_k := p_k^{(1)}$. For the weak measurement $\hat{M}^{(k)}_{-|\{p_k^{(1)},\vec{s}_k\}}$ for -1 outcome, the same result of $r_k^{(n)}$ is obtained. Then, the total reversibility $R(N)$ of a photon pair by multiple reversal measurements applied up to N times for each of Alice and Bob is

$$\begin{aligned} R(N) &= \sum_{n=1}^{N} 2r_A^{(n)} \sum_{m=1}^{N} 2r_B^{(m)} \\ &= \prod_{k=A,B} p_k \left\{ \coth\left(2^{-1} \ln\left(\frac{1+p_k}{1-p_k}\right)\right) - \coth\left(2^{N-1} \ln\left(\frac{1+p_k}{1-p_k}\right)\right) \right\}. \end{aligned} \tag{S3}$$

The reversibility by a single reversal measurement is $R(1) = (1-p_A^2)(1-p_B^2)/4$ (agreeing with the main text), and the maximum reversibility is $R(\infty) = (1-p_A)(1-p_B)$, obtained by the infinite number of reversal measurements.

In Fig. S6A, we compare the maximum reversibility $R(\infty)$ and the reversibility by a single reversal measurement $R(1)$. Note that approaching the maximum reversibility $R(\infty)$ does not in fact require a large number of reversal measurements. For example, Fig. S6B demonstrates that only two reversal measurements are already good for the Bell nonlocality test, and similarly, five reversal measurements for the steering test.

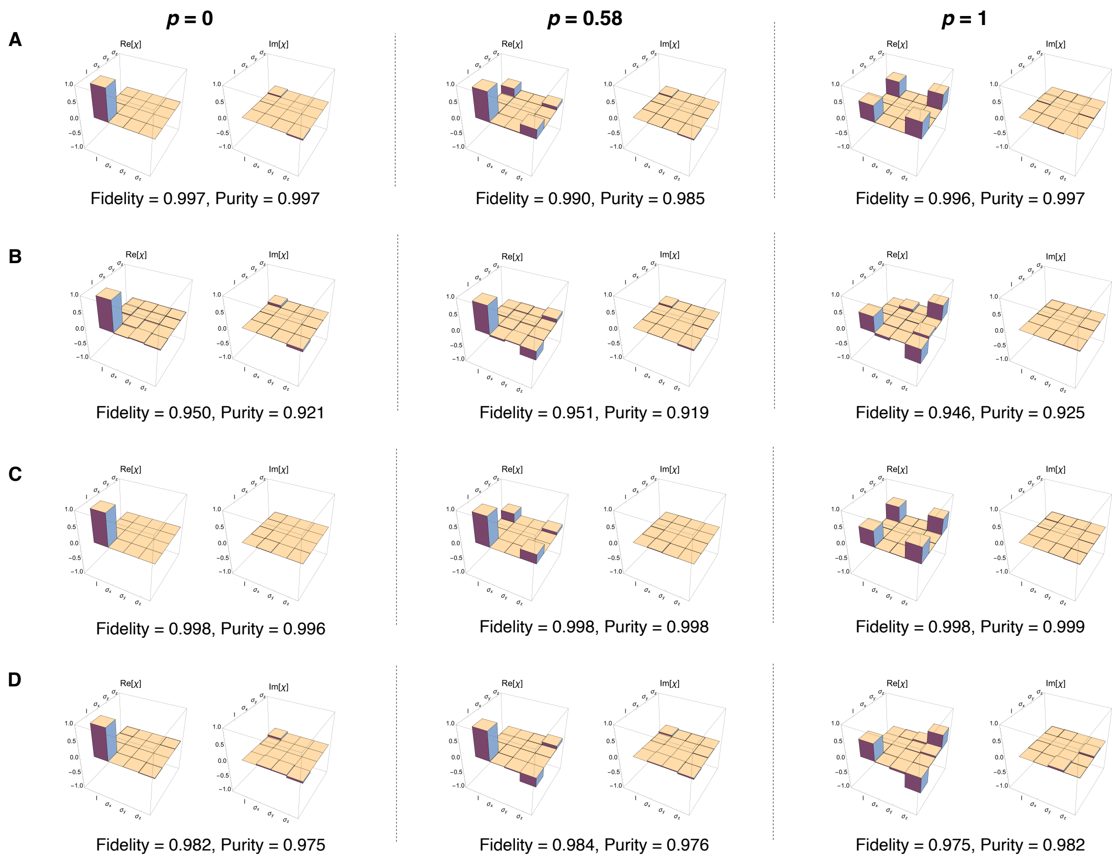

Fig. S1: **Quantum process tomography of weak measurements.** Alice's weak measurement for (**A**) + output ($\hat{M}^{(A)}_{+|\{p,\vec{z}\}}$) and (**B**) $-$ output ($\hat{M}^{(A)}_{-|\{p,\vec{z}\}}$). Bob's weak measurement for (**C**) + output ($\hat{M}^{(B)}_{+|\{p,\vec{z}\}}$) and (**D**) $-$ output ($\hat{M}^{(B)}_{-|\{p,\vec{z}\}}$). Measurement strengths are $p = 0$ (left), $p = 0.58$ (middle), and $p = 1$ (right).

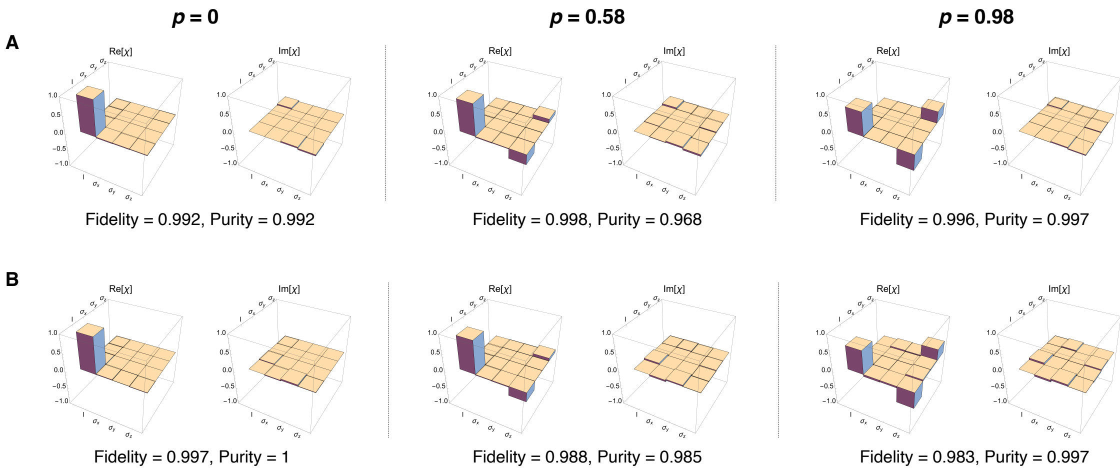

Fig. S2: **Quantum process tomography of reversal measurements.** Alice's reversal measurement ($\hat{R}^{(A)}_{+|\{p,\vec{z}\}}$), (**B**) Bob's reversal measurement ($\hat{R}^{(B)}_{+|\{p,\vec{z}\}}$). Measurement strengths are $p = 0$ (left), $p = 0.58$ (middle), and $p = 0.98$ (right). Note that p =1 has no reversal measurement since it corresponds to a projective measurement.

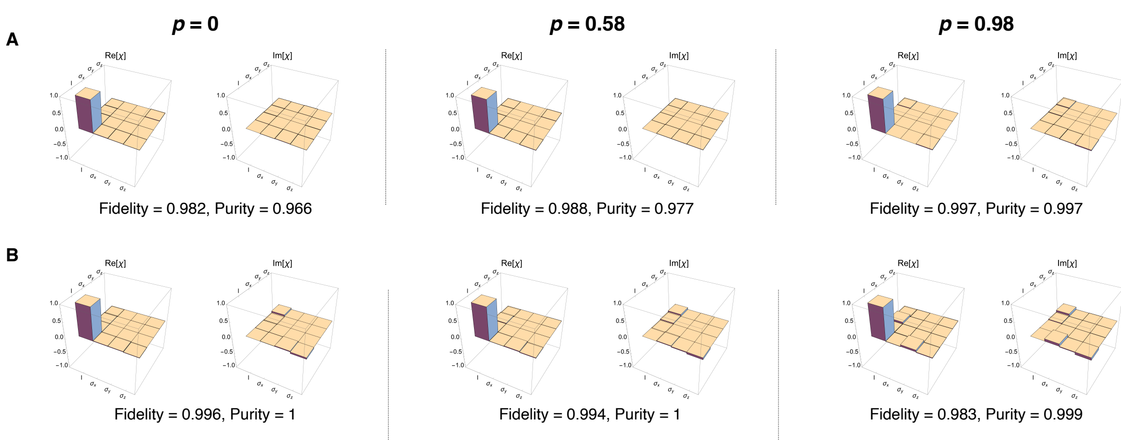

Fig. S3: **Quantum process tomography of weak and reversal measurements.** The results for (**A**) Alice's side ($\hat{R}^{(A)}_{+|\{p,\vec{z}\}}\hat{M}^{(A)}_{+|\{p,\vec{z}\}}$) and (**B**) Bob's side ($\hat{R}^{(B)}_{+|\{p,\vec{z}\}}\hat{M}^{(B)}_{+|\{p,\vec{z}\}}$). Measurement strengths are $p = 0$ (left), $p = 0.58$ (middle), and $p = 0.98$ (right).

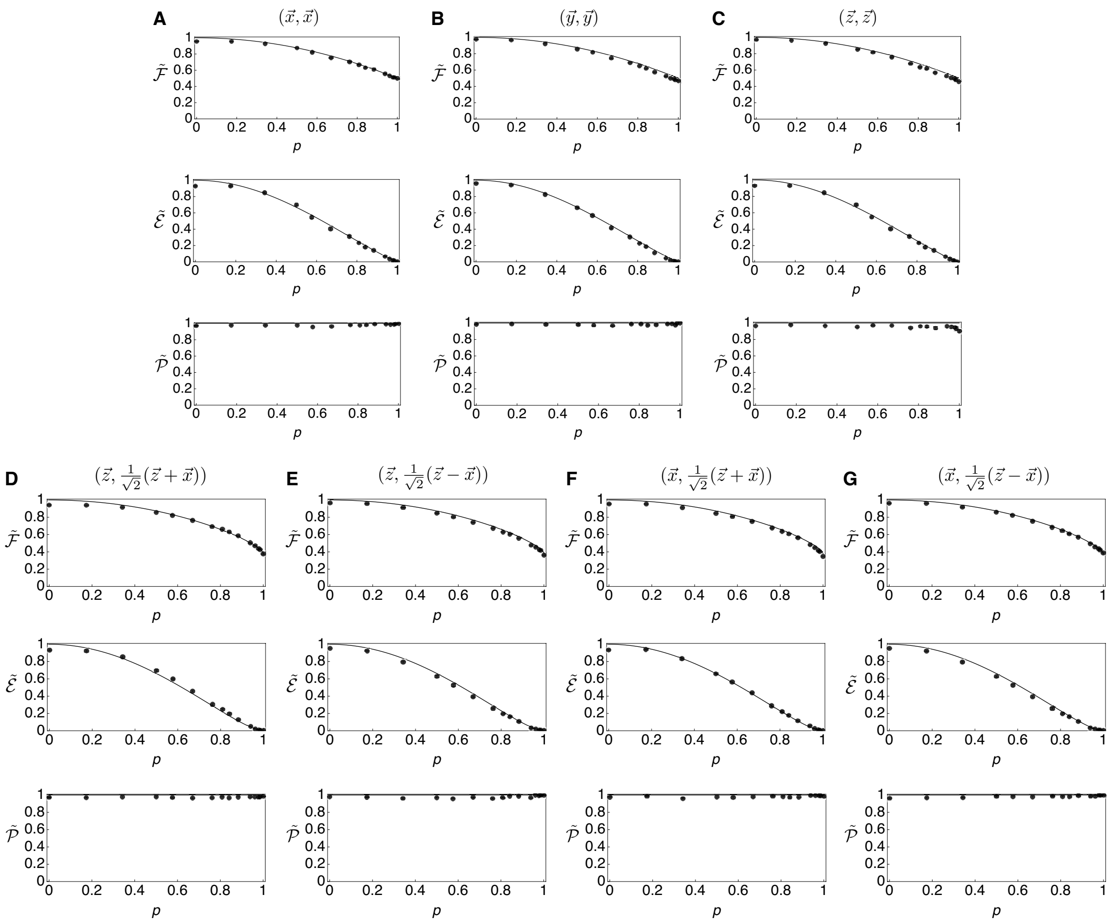

Fig. S4: **Properties of quantum states after weak measurement.** Average properties of quantum states after weak measurement are plotted for each measurement direction $\vec{r}_A$ and $\vec{r}_B$ (average fidelity $\tilde{\mathcal{F}}_{(\vec{r}_A,\vec{r}_B)}$, average entanglement of formation $\tilde{\mathcal{E}}_{(\vec{r}_A,\vec{r}_B)}$, and average purity $\tilde{\mathcal{P}}_{(\vec{r}_A,\vec{r}_B)}$). The average is mathematically defined as $\tilde{\mathcal{Q}}_{(\vec{r}_A,\vec{r}_B)} = \sum_{l_A=\pm1}\sum_{l_B=\pm1} P(l_A, l_B|\vec{r}_A, \vec{r}_B)\ \mathcal{Q}\left[\rho_m\right]$. The measurement directions are (**A**) $\vec{r}_A = \vec{x}$, $\vec{r}_B = \vec{x}$, (**B**) $\vec{r}_A = \vec{y}$, $\vec{r}_B = \vec{y}$ (**C**) $\vec{r}_A = \vec{z}$, $\vec{r}_B = \vec{z}$, (**D**) $\vec{r}_A = \vec{z}$, $\vec{r}_B = \frac{1}{\sqrt{2}}(\vec{z}+\vec{x})$, (**E**) $\vec{r}_A = \vec{z}$, $\vec{r}_B = \frac{1}{\sqrt{2}}(\vec{z}-\vec{x})$, (**F**) $\vec{r}_A = \vec{x}$, $\vec{r}_B = \frac{1}{\sqrt{2}}(\vec{z}+\vec{x})$, and (**G**) $\vec{r}_A = \vec{x}$, $\vec{r}_B = \frac{1}{\sqrt{2}}(\vec{z}-\vec{x})$. Dots and lines are the experimental data and the theory graphs by the ideal condition, respectively. Error bars, which are smaller than the dot size, denote one standard deviation.

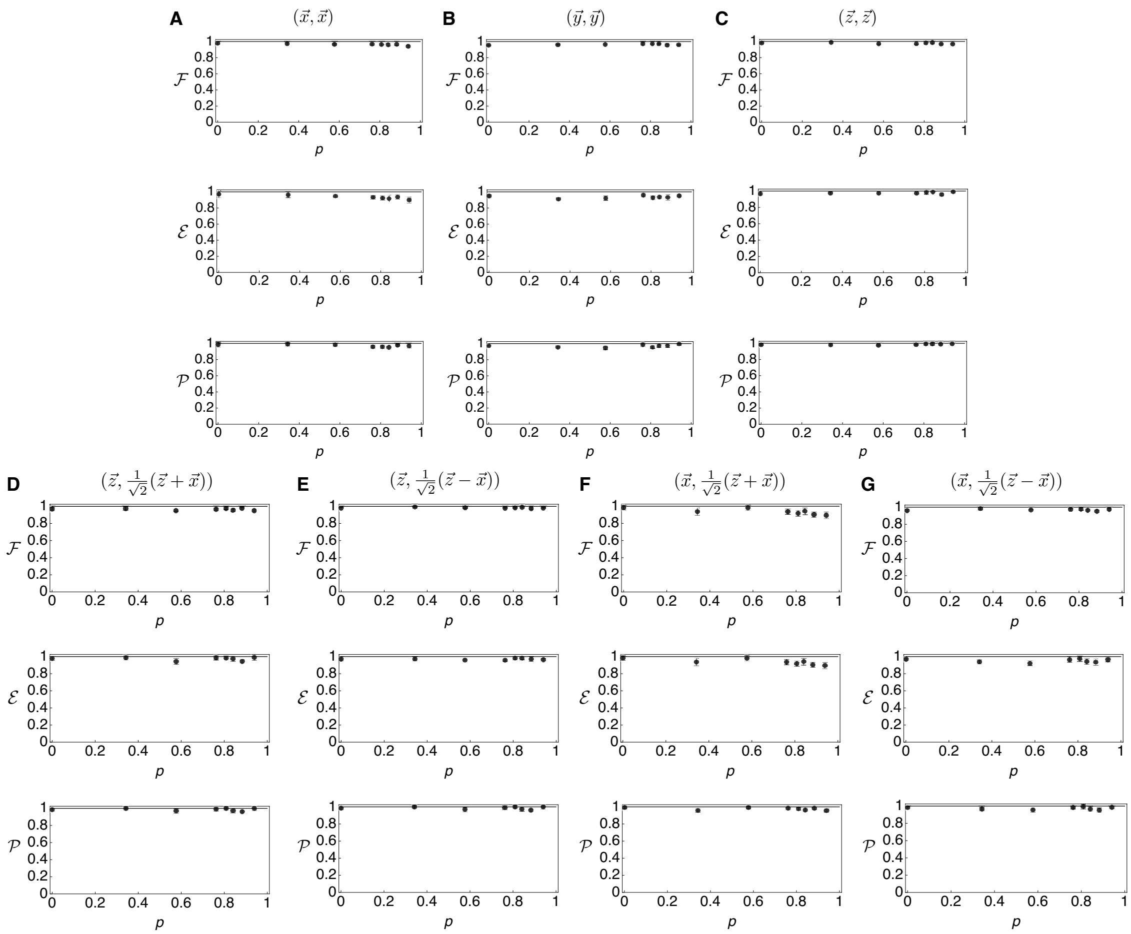

Fig. S5: **Properties of quantum states after weak and reversal measurements.** For weak measurements $\hat{M}^{(A)}_{+|\{p,\vec{r}_A\}}$ and $\hat{M}^{(B)}_{+|\{p,\vec{r}_B\}}$, we apply the corresponding reversal measurements $\hat{R}^{(A)}_{+|\{p,\vec{r}_A\}}$ and $\hat{R}^{(B)}_{+|\{p,\vec{r}_B\}}$, respectively. The properties of each resulting state is plotted ($\mathcal{F}$: fidelity, $\mathcal{E}$: entanglement of formation, $\mathcal{P}$: purity). The measurement directions are (**A**) $\vec{r}_A = \vec{x}$, $\vec{r}_B = \vec{x}$, (**B**) $\vec{r}_A = \vec{y}$, $\vec{r}_B = \vec{y}$, (**C**) $\vec{r}_A = \vec{z}$, $\vec{r}_B = \vec{z}$, (**D**) $\vec{r}_A = \vec{z}$, $\vec{r}_B = \frac{1}{\sqrt{2}}(\vec{z}+\vec{x})$, (**E**) $\vec{r}_A = \vec{z}$, $\vec{r}_B = \frac{1}{\sqrt{2}}(\vec{z}-\vec{x})$, (**F**) $\vec{r}_A = \vec{x}$, $\vec{r}_B = \frac{1}{\sqrt{2}}(\vec{z}+\vec{x})$, and (**G**) $\vec{r}_A = \vec{x}$, $\vec{r}_B = \frac{1}{\sqrt{2}}(\vec{z}-\vec{x})$. Dots and lines are the experimental data and the theory graphs by the ideal condition, respectively. Error bars denote one standard deviation.

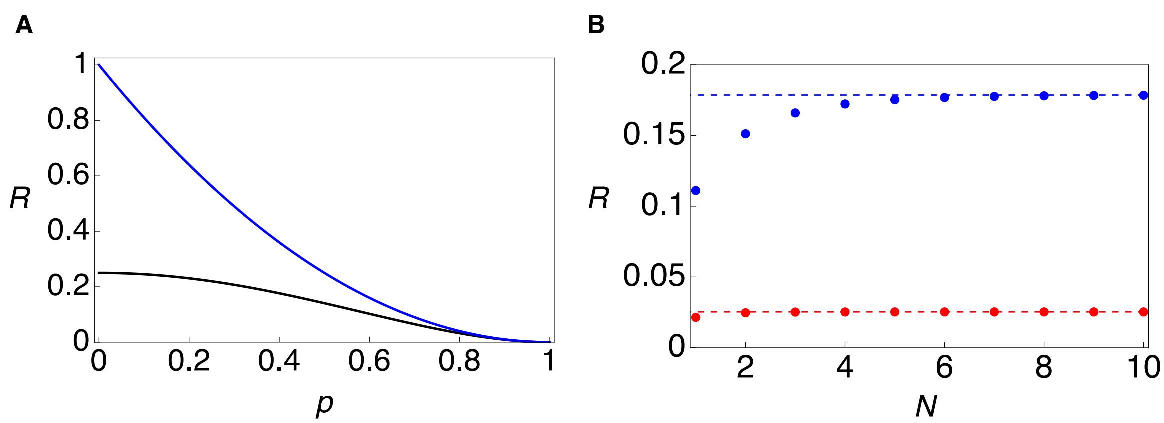

Fig. S6: **Improving reversibility by multiple reversal measurements.** (**A**) The blue line represents the reversibility by the infinite number of reversal measurements, $R(\infty) = (1-p)^2$, and the black line represents the reversibility by a single reversal measurement, $R(1) = (1-p^2)^2/4$. We use the same measurement strength $p_A = p_B = p$. (**B**) Reversibility as a function of the number N of reversal measurements employed, $R(N)$. Only few applications of reversal measurements (dot) already give reversibility that approaches the maximum reversibility (dotted line). The reversibility is calculated for the minimum measurement strength required for the steering test ($p_A = p_B = 3^{-1/2}$, Blue) and for the minimum strength required for the Bell nonlocality test ($p_A = p_B = 2^{-1/4}$, Red).

REFERENCES AND NOTES

1. A. K. Ekert, Quantum cryptography based on Bell's theorem. *Phys. Rev. Lett.* **67**, 661–663 (1991).

2. W. Zhang, D.-S. Ding, Y.-B. Sheng, L. Zhou, B.-S. Shi, G.-C. Guo, Quantum secure direct communication with quantum memory. *Phys. Rev. Lett.* **118**, 220501 (2017).

3. J.-G. Ren, P. Xu, H.-L. Yong, L. Zhang, S.-K. Liao, J. Yin, W.-Y. Liu, W.-Q. Cai, M. Yang, L. Li, K.-X. Yang, X. Han, Y.-Q. Yao, J. Li, H.-Y. Wu, S. Wan, L. Liu, D.-Q. Liu, Y.-W. Kuang, Z.-P. He, P. Shang, C. Guo, R.-H. Zheng, K. Tian, Z.-C. Zhu, N.-L. Liu, C.-Y. Lu, R. Shu, Y.-A. Chen, C.-Z. Peng, J.-Y. Wang, J.-W. Pan, Ground-to-satellite quantum teleportation. *Nature* **549**, 70–73 (2017).

4. T. Darras, B. E. Asenbeck, G. Guccione, A. Cavaillès, H. Le Jeannic, J. Laurat, A quantum-bit encoding converter. *Nat. Photon.* **17**, 165–170 (2023).

5. X. Guo, C. R. Breum, J. Borregaard, S. Izumi, M. V. Larsen, T. Gehring, M. Christandl, J. S. Neergaard-Nielsen, U. L. Andersen, Distributed quantum sensing in a continuous-variable entangled network. *Nat. Phys.* **16**, 281–284 (2020).

6. L.-Z. Liu, Y.-Z. Zhang, Z.-D. Li, R. Zhang, X.-F. Yin, Y.-Y. Fei, L. Li, N.-L. Liu, F. Xu, Y.-A. Chen, J.-W. Pan, Distributed quantum phase estimation with entangled photons. *Nat. Photon.* **15**, 137–142 (2021).

7. M. V. Larsen, X. Guo, C. R. Breum, J. S. Neergaard-Nielsen, U. L. Andersen, Deterministic multi-mode gates on a scalable photonic quantum computing platform. *Nat. Phys.* **17**, 1018–1023 (2021).

8. L. S. Madsen, F. Laudenbach, M. F. Askarani, F. Rortais, T. Vincent, J. F. F. Bulmer, F. M. Miatto, L. Neuhaus, L. G. Helt, M. J. Collins, A. E. Lita, T. Gerrits, S. W. Nam, V. D. Vaidya, M. Menotti, I. Dhand, Z. Vernon, N. Quesada, J. Lavoie, Quantum computational advantage with a programmable photonic processor. *Nature* **606**, 75–81 (2022).

9. N. Friis, G. Vitagliano, M. Malik, M. Huber, Entanglement certification from theory to experiment. *Nat. Rev. Phys.* **1**, 72–87 (2019).

10. J. Eisert, D. Hangleiter, N. Walk, I. Roth, D. Markham, R. Parekh, U. Chabaud, E. Kashefi, Quantum certification and benchmarking. *Nat. Rev. Phys.* **2**, 382–390 (2020).

11. D. F. V. James, P. G. Kwiat, W. J. Munro, A. G. White, Measurement of qubits. *Phys. Rev. A* **64**, 052312 (2001).

12. O. Guhne, P. Hyllus, D. Bruß, A. Ekert, M. Lewenstein, C. Macchiavello, A. Sanpera, Detection of entanglement with few local measurements. *Phys. Rev. A* **66**, 062305 (2002).

13. D. J. Saunders, S. J. Jones, H. M. Wiseman, G. J. Pryde, Experimental EPR-steering using Bell-local states. *Nat. Phys.* **6**, 845–849 (2010).
14. L. K. Shalm, E. Meyer-Scott, B. G. Christensen, P. Bierhorst, M. A. Wayne, M. J. Stevens, T. Gerrits, S. Glancy, D. R. Hamel, M. S. Allman, K. J. Coakley, S. D. Dyer, C. Hodge, A. E. Lita, V. B. Verma, C. Lambrocco, E. Tortorici, A. L. Migdall, Y. Zhang, D. R. Kumor, W. H. Farr, F. Marsili, M. D. Shaw, J. A. Stern, C. Abellán, W. Amaya, V. Pruneri, T. Jennewein, M. W. Mitchell, P. G. Kwiat, J. C. Bienfang, R. P. Mirin, E. Knill, S. W. Nam, Strong loophole-free test of local realism. *Phys. Rev. Lett.* **115**, 250402 (2015).
15. M. Giustina, M. A. M. Versteegh, S. Wengerowsky, J. Handsteiner, A. Hochrainer, K. Phelan, F. Steinlechner, J. Kofler, J.-A. Larsson, C. Abellán, W. Amaya, V. Pruneri, M. W. Mitchell, J. Beyer, T. Gerrits, A. E. Lita, L. K. Shalm, S. W. Nam, T. Scheidl, R. Ursin, B. Wittmann, A. Zeilinger, Significant-loophole-free test of bell's theorem with entangled photons. *Phys. Rev. Lett.* **115**, 250401 (2015).
16. B. Hensen, H. Bernien, A. E. Dréau, A. Reiserer, N. Kalb, M. S. Blok, J. Ruitenberg, R. F. L. Vermeulen, R. N. Schouten, C. Abellán, W. Amaya, V. Pruneri, M. W. Mitchell, M. Markham, D. J. Twitchen, D. Elkouss, S. Wehner, T. H. Taminiau, R. Hanson, Loophole-free Bell inequality violation using electron spins separated by 1.3 kilometres. *Nature* **526**, 682–686 (2015).
17. K. Banaszek, Fidelity balance in quantum operations. *Phys. Rev. Lett.* **86**, 1366–1369 (2001).
18. H.-T. Lim, Y.-S. Ra, K. H. Hong, S. W. Lee, Y.-H. Kim, Fundamental bounds in measurements for estimating quantum states. *Phys. Rev. Lett.* **113**, 020504 (2014).
19. R. Silva, N. Gisin, Y. Guryanova, S. Popescu, Multiple observers can share the nonlocality of half of an entangled pair by using optimal weak measurements. *Phys. Rev. Lett.* **114**, 250401 (2015).
20. T. C. White, J. Y. Mutus, J. Dressel, J. Kelly, R. Barends, E. Jeffrey, D. Sank, A. Megrant, B. Campbell, Y. Chen, Z. Chen, B. Chiaro, A. Dunsworth, I.-C. Hoi, C. Neill, P. J. J. O'Malley, P. Roushan, A. Vainsencher, J. Wenner, A. N. Korotkov, J. M. Martinis, Preserving entanglement during weak measurement demonstrated with a violation of the Bell–Leggett–Garg inequality. *npj Quantum Inf.* **2**, 15022 (2016).
21. M.-J. Hu, Z.-Y. Zhou, X.-M. Hu, C.-F. Li, G.-C. Guo, Y.-S. Zhang, Observation of non-locality sharing among three observers with one entangled pair via optimal weak measurement. *npj Quantum Inf.* **4**, 63 (2018).

22. G. Foletto, L. Calderaro, A. Tavakoli, M. Schiavon, F. Picciariello, A. Cabello, P. Villoresi, G. Vallone, Experimental certification of sustained entanglement and nonlocality after sequential measurements. *Phys. Rev. Appl.* **13**, 044008 (2020).

23. Y.-H. Choi, S. Hong, T. Pramanik, H.-T. Lim, Y.-S. Kim, H. Jung, S.-W. Han, S. Moon, Y.-W. Cho, Demonstration of simultaneous quantum steering by multiple observers via sequential weak measurements. *Optica* **7**, 675–679 (2020).

24. S. Hong, Y.-S. Kim, Y.-W. Cho, J. Kim, S.-W. Lee, H.-T. Lim, Demonstration of complete information trade-off in quantum measurement. *Phys. Rev. Lett.* **128**, 050401 (2022).

25. J. Zhu, M.-J. Hu, C.-F. Li, G.-C. Guo, Y.-S. Zhang, Einstein-Podolsky-Rosen steering in two-sided sequential measurements with one entangled pair. *Phys. Rev. A* **105**, 032211 (2022).

26. Y.-S. Kim, Y.-W. Cho, Y.-S. Ra, Y.-H. Kim, Reversing the weak quantum measurement for a photonic qubit. *Opt. Express* **17**, 11978–11985 (2009).

27. Y.-S. Kim, J.-C. Lee, O. Kwon, Y.-H. Kim, Protecting entanglement from decoherence using weak measurement and quantum measurement reversal. *Nat. Phys.* **8**, 117–120 (2012).

28. N. Brunner, D. Cavalcanti, S. Pironio, V. Scarani, S. Wehner, Bell nonlocality. *Rev. Mod. Phys.* **86**, 419–478 (2014).

29. V. Händchen, T. Eberle, S. Steinlechner, A. Samblowski, T. Franz, R. F. Werner, R. Schnabel, Observation of one-way Einstein–Podolsky–Rosen steering. *Nat. Photon.* **6**, 596–599 (2012).

30. J. Bowles, T. Vértesi, M. T. Quintino, N. Brunner, One-way Einstein-Podolsky-Rosen steering. *Phys. Rev. Lett.* **112**, 200402 (2014).

31. Y.-H. Kim, S. P. Kulik, M. V. Chekhova, W. P. Grice, Y. Shih, Experimental entanglement concentration and universal Bell-state synthesizer. *Phys. Rev. A* **67**, 010301 (2003).

32. J. Eisert, F. G. S. L. Brandão, K. M. R. Audenaert, Quantitative entanglement witnesses. *New J. Phys.* **9**, 46 (2007).

33. O. Gühne, M. Reimpell, R. F. Werner, Estimating entanglement measures in experiments. *Phys. Rev. Lett.* **98**, 110502 (2007).

34. B. W. Reichardt, F. Unger, U. Vazirani, Classical command of quantum systems. *Nature* **496**, 456–460 (2013).

35. P. Bierhorst, E. Knill, S. Glancy, Y. Zhang, A. Mink, S. Jordan, A. Rommal, Y.-K. Liu, B. Christensen, S. W. Nam, M. J. Stevens, L. K. Shalm, Experimentally generated randomness certified by the impossibility of superluminal signals. *Nature* **556**, 223–226 (2018).

36. W.-Z. Liu, Y.-Z. Zhang, Y.-Z. Zhen, M.-H. Li, Y. Liu, J. Fan, F. Xu, Q. Zhang, J.-W. Pan, Toward a photonic demonstration of device-independent quantum key distribution. *Phys. Rev. Lett.* **129**, 050502 (2022).
37. W. Zhang, T. van Leent, K. Redeker, R. Garthoff, R. Schwonnek, F. Fertig, S. Eppelt, W. Rosenfeld, V. Scarani, C. C. W. Lim, H. Weinfurter, A device-independent quantum key distribution system for distant users. *Nature* **607**, 687–691 (2022).
38. Y. Pan, J. Zhang, E. Cohen, C.-W. Wu, P.-X. Chen, N. Davidson, Weak-to-strong transition of quantum measurement in a trapped-ion system. *Nat. Phys.* **16**, 1206–1210 (2020).
39. S. M. Lee, H. Kim, M. Cha, H. S. Moon, Polarization-entangled photon-pair source obtained via type-II non-collinear SPDC process with PPKTP crystal. *Opt. Express* **24**, 2941–2953 (2016).
40. Y.-C. Jeong, K.-H. Hong, Y.-H. Kim, Bright source of polarization-entangled photons using a PPKTP pumped by a broadband multi-mode diode laser. *Opt. Express* **24**, 1165–1174 (2016).
41. J. Fiurášek, Z. Hradil, Maximum-likelihood estimation of quantum processes. *Phys. Rev. A* **63**, 020101 (2001).